

# Volume Measurement System Based on Hall Effect Sensors Circularly Coupled and Arranged in a Quadrature Shape

Juan Carlos Martínez Espinosa<sup>1</sup>, Juan de Dios Ortiz Alvarado<sup>1</sup>, Fidel Córdoba Valdes<sup>1</sup>,  
Marcos Alberto Rodríguez Martínez<sup>1</sup>, Marcos Leonardo Fuentes Avila<sup>1</sup>,  
Rafael Guzmán Cabrera<sup>2</sup>

<sup>1</sup> Instituto Politécnico Nacional,  
Unidad Profesional Interdisciplinaria de Ingeniería, Campus Guanajuato,  
Mexico

<sup>2</sup> Universidad de Guanajuato, campus Irapuato,  
Departamento de Ingeniería Eléctrica,  
Mexico

{jcmartineze, jdortiza, fcordovav}@ipn.mx,  
{mrodriguez1604, mfuentes1700}@alumnoipn.mx,  
guzmanc@ugto.mx

**Abstract:** In this research work, a compact electronic system for measuring volumes in generic cylindrical containers was designed and developed. The system is based on a circular arrangement composed of four Hall effect sensors A1324 and arranged in the form of a quadrature. The theoretical volume calculations obtained based on the angle of inclination of the float for a cylindrical container were correlated with a polynomial function of order 3 with an  $R^2 = 0.99$ . The analog voltage signal correlated with the theoretical volume was digitized through a microcontroller and a ZigBee transceiver was used as a data transmission channel and through a ZigBee Xbee ZB24 transceiver was used for information transfer. The experimental and theoretical results obtained corroborate a highly accurate and reliable measurement system, which can be applied to different containers and different types of fluids that are to be monitored remotely. Finally based on the theoretical model, this system could be scaled to cylindrical containers of greater capacity without modifying the conditions of the electronic system with the array of Hall effect sensors.

**Keywords:** Magnetic sensor, Hall effect, volume measurement, ZigBee protocol.

## 1 Introduction

Currently sensory devices have been used for different detection systems, as well as for remote monitoring in different applications are also widely used, which range from simple temperature monitoring, to nanometric detection of angular positioning [1-5]. Researchers from different parts of the world have developed and implemented new methodologies for the detection of certain physical variables through the basic science applied to generate new utility models as intelligent devices that favor the detection, monitoring and therefore the control of various industrial processes [6-11].

Highly reliable and very precise sensory devices are also those sensors that are based on the modification of a magnetic field to correlate it to a physical variable, as long as this process linked to a conditioning and calibration of the signal without disturbances of any noise source [12].

Some sensors of this type have been used for air navigation, applications in the automotive industry and in agriculture [13, 14], in other cases they have been applied for the monitoring of ferromagnetic particles generated by wear of any



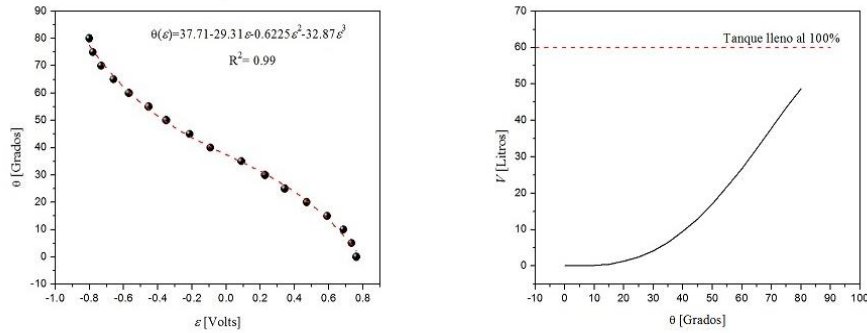


**Fig. 3.** Behavior of the readings and adjustment function found. (a) Adjust to a polynomial of order 3 for experimental angle data as a function of voltage, (b) Theoretical volume behavior as a function of angle

**Table 1.** Voltage readings recorded from the triplicate detection system. Abbreviations are as follows,  $\theta$ : float angle,  $\epsilon$ : measurement system voltage,  $\mu$ : arithmetic mean,  $\sigma$ : standard deviation

$\theta$	$\epsilon_1$	$\epsilon_2$	$\epsilon_3$	$\mu$	$\sigma$
0	0.755	0.77	0.762	0.762	0.008
5	0.74	0.739	0.721	0.733	0.011
10	0.709	0.687	0.665	0.687	0.022
15	0.625	0.589	0.558	0.591	0.034
20	0.49	0.465	0.461	0.472	0.016
25	0.362	0.332	0.333	0.342	0.017
30	0.29	0.196	0.199	0.228	0.053
35	0.18	0.04	0.047	0.089	0.079
40	-0.095	-0.064	-0.118	-0.092	0.027
45	-0.184	-0.221	-0.235	-0.213	0.026
50	-0.326	-0.357	-0.368	-0.350	0.022
55	-0.43	-0.458	-0.473	-0.454	0.022
60	-0.581	-0.548	-0.578	-0.569	0.018
65	-0.657	-0.645	-0.676	-0.659	0.016
70	-0.75	-0.712	-0.73	-0.731	0.019
75	-0.792	-0.772	-0.773	-0.779	0.011
80	-0.813	-0.797	-0.793	-0.801	0.011

**2.2. Theoretical Calculations and System Calibration**

differential volume element is given by the following expression (Eq. 1):

$$dV = L(2y)dy, \tag{1}$$

A system based on a cylinder with the dimensions shown in Figure 2b was used. The volume of a cylinder whose base is the semicircular region shown in Figure 2a is calculated. Where the

where  $x = \sqrt{R^2 - y^2}$ . And the limits are:  $-R$  y  $-R+h$ , this way we have to:

$$V = \int dV, \quad (2)$$

$$V = \int_{-R}^{-R+h} 2L\sqrt{R^2 - y^2} dy, \quad (3)$$

$$V = L \left[ \frac{\pi}{2} R^2 + (h - R) \sqrt{2Rd - d^2} + R^2 \operatorname{sen}^{-1} \left( \frac{h}{R} - 1 \right) \right]. \quad (4)$$

The voltage records to obtain the behavior of the float angle versus the voltage that the system emits, were carried out in triplicate. Its arithmetic mean and standard deviation of the readings were determined.

### 2.3 Data Analysis and Acquisition Software

The MPLABX development environment was used for the firmware implementation of the microcontroller responsible for the acquisition, and signal processing. For theoretical and experimental analysis, software tools such as SolidWorks v2018, Mathematica 10.0, Matlab R2015b and OriginLab v 8.0 were used.

## 3 Results and Discussion

For the determination of the volume contained in the cylinder as a function of the angle  $\theta$  shown in Figure 2B, we note that:

$$h = 2R - (a + b \cos \theta). \quad (5)$$

Taking Eq. (5) and substituting in Eq. (4), the volume of the cylindrical container was obtained as a function of the angle (Eq. (6)). Where  $\theta$  must be expressed in radians:

$$V = L \left[ R^2 \cos^{-1} \left( \frac{a + b \cos \theta - R}{R} \right) - (a + b \cos \theta - R) \sqrt{(2R - a - b \cos \theta)(a + b \cos \theta)} \right]. \quad (6)$$

Experimentally, the angle was measured as a function of the voltage ( $\varepsilon$ ). Table 1 summarizes the recorded readings, and where we can verify the angle and voltage correlation.

The behavior of the experimental measurements is shown in Figure 3A, where the

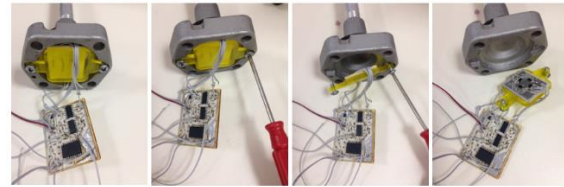


**Fig. 4.** Mounting the measuring hardware on the mechanical base that supports the float arm

spherical symbols represent the experimental data and the solid dotted line is an adjustment of a polynomial of order 3. The polynomial that best fitted this behavior was:

$$\theta(\varepsilon) = 37.71 - 29.31 \varepsilon - 0.6225 \varepsilon^2 - 32.87 \varepsilon^3. \quad (7)$$

It is important to note that this last expression allows us to calculate the angle in degrees as a function of voltage. On the other hand, in Eq. (6) the angle in radians is required, therefore, Eq. (7) must be multiplied by a factor  $\pi/180$ .

Finally, substituting Eq. (7) in Eq. (6) we obtain the volume as a function of the voltage recorded by our remote system (Figure 3b).

In Figure 4, the printed circuits corresponding to the sensing stages (arrangement of the 4 Hall-effect sensors A1324 in the form of quadrature) and signal conditioning are observed.

## 4 Conclusions

In this paper, a liquid volume measurement system of a container was developed by monitoring the magnetic field strength to determine the position of a float. This system, unlike those based on variable resistance measurement, does not show loss of accuracy caused by transducer wear; and with respect to those that use ultrasonic sensor, errors in the measurement by reflection of ultrasonic beam in the walls of the tank are avoided when this is very narrow.

The electronic hardware is compact allowing its coupling to the mechanical system of the float arm, and together with the Zigbee transceiver, it allows to have a very complete measurement system with low energy consumption and compatible for integration as part of a variable measurement network.

On the other hand, the correlation of the angular position of the float arm with the contained volume was also determined. This correlation function can be applied to systems such as the one described above and when the dimensions of the cylindrical container and the length of the float arm are defined. The mathematical expression to determine the content volume can be implemented in the microcontroller firmware. Finally, this detection system can be coupled to different cylindrical tanks, as long as their dimensions for a, b, R and L are modified proportionally and in addition to their firmware update for these constants.

## Acknowledgments

We thank the IPN research and postgraduate secretary for partial financial support through the SIP 2019004 and SIP 20200637 projects.

## References

- Rai., V.K. (2007).** Temperature sensors and optical sensors. *Applied Physics B*, Vol. 88, pp. 297–303. DOI: 10.1007/s00340-007-2717-4.
- Lee, J., Kwon, H., Seo, J., Shin, S., Koo, J.H., Pang, C., Son, S., Kim, J.H., Jang, Y.H., Kim, D.E. (2015).** Conductive fiber-based ultrasensitive textile pressure sensor for wearable electronics. *Advanced Materials*, Vol. 27, pp. 2433–2439. DOI: 10.1002/adma. 201500009.
- Back, J.A., Tedesco, L.P., Molz, R.F., Nara, E.O.B. (2016).** An embedded system approach for energy monitoring and analysis in industrial processes. *Energy*, Vol. 115, No. 1, pp. 811–819. DOI: 10.1016/j.energy.2016. 09.045.
- Chung, Y.-C., Chuang, S.-T., Chen, T.-Y., Lo, C.-Y., Chen, R. (2016).** Capacitive tactile sensor for angle detection and its accuracy study. *IEEE Sensors Journal*, Vol. 16, No. 18, pp. 6857–6865. DOI: 10.1109/JSEN. 2016.25 83544.
- Ma, M., Chen, H., Li, S., Jing, X., Zhang, W., Liu, Y., Zhu, E. (2019).** Highly sensitive temperature sensor based on Sagnac interferometer with liquid crystal photonic crystal fibers. *Optik International Journal for Light and Electron Optics*, Vol. 179, pp. 665–671. DOI: 10.1016/j.ijleo.2018.11.006.
- Espejo, A., Tejo, F., Vidal-Silva, N., Escrig, J. (2017).** Nanometric alternating magnetic field generator. *Scientific Reports*, Vol. 7, No. 1, pp. 1–7. DOI: 10.1038/s41598-017-050 26- 4.
- Malek, B.S., Pagel, Z., Wu, X., Müller, H. (2019).** Embedded control system for mobile atom interferometers. *Review of Scientific Instruments*, Vol. 90, No. 7, pp. 073103. DOI: 10.1063/1.5083981.
- Lee, S., Reuveny, A., Reeder, J., Lee, S., Jin, H., Liu, Q., Yokota, T., Sekitani, T., Isoyama, T., Abe, Y. (2016).** A transparent bending-insensitive pressure sensor. *Nature Nanotechnology*, Vol. 11, No. 5, pp. 472–478. DOI: 10.1038/nnano. 2015.324.
- Yin, Z., Hou, J. (2016).** Recent advances on SVM based fault diagnosis and process monitoring in complicated industrial processes. *Neurocomputing*, Vol. 174, pp. 643–650. DOI: 10.1016/j.neucom.2015.09. 081.
- Han, S., Kim, J., Won, S.M., Ma, Y., Kang, D., Xie, Z., Lee, K.-T., Chung, H.U., Banks, A., Min, S. (2018).** Battery-free, wireless sensors for full-body pressure and temperature mapping. *Science Translational Medicine*, Vol. 10, No. 435. DOI: 10.1126/ scitranslmed.aan4950.
- Behan, M., Krejcar, O., Sabbah, T., Selamat, A. (2019).** Sensorial network framework embedded in ubiquitous mobile devices. *Future Internet*, Vol. 11, No. 10, pp. 215. DOI: 10.3390/fi11100215.
- Lenz, J., Edelstein, S. (2006).** Magnetic sensors and their applications. *IEEE Sensors Journal*, Vol. 6, No. 3, pp. 631–649. DOI: 10.1109/JSEN. 2006.874493.
- Treutler, C. (2001).** Magnetic sensors for automotive applications. *Sensors and Actuators A: Physical*, Vol. 91, No. 1-2, pp. 2–6. DOI: 10.1016/S0924-4247(01)00621-5.
- Bogue, R. (2017).** Sensors key to advances in precision agriculture. *Sensor Review*, Vol. 37, No. 1, pp. 1–6. DOI:10.1108/SR-10-2016-0215.
- Jia, R., Ma, B., Zheng, C., Wang, L., Ba, X., Du, Q., Wang, K. (2018).** Magnetic properties of ferromagnetic particles under alternating magnetic fields: Focus on particle detection sensor applications. *Sensors*, Vol. 18, No. 12, pp. 4144. DOI: 10.3390/s18124144.
- Jogschies, L., Klaas, D., Kruppe, R., Rittinger, J., Taptimthong, P., Wienecke, A., Rissing, L., Wurz, M.C. (2015).** Recent developments of magnetoresistive sensors for industrial applications. *Sensors*, Vol. 15, No. 11, pp. 28665–28689. DOI: 10.3390/ s151128665.

17. **Zhang, W., Pan, Z., Zhou, H., Wang, E., (2017).** A novel micro-magnetic sensor based on GMI effect. AIP Conference Proceedings, AIP Publishing LLC, pp. 020099. DOI: 10.1063/1.4982464.
18. **Joh, H., Yang, I., Ryoo, I. (2016).** The internet of everything based on energy efficient P2P transmission technology with Bluetooth low energy. Peer-to-Peer Networking and Applications, Vol. 9, No. 3, pp. 520–528. DOI: 10.1007/s12083-015-0377-4.
19. **Shariff, F., Abd-Rahim, N., Hew, W.P. (2015).** Zigbee-based data acquisition system for online monitoring of grid-connected photovoltaic system. Expert Systems with Applications, Vol. 42, No. 3, pp. 1730–1742. DOI: 10.1016/j.eswa.2014.10.007.
20. **Liu, Z.-y. (2014).** Hardware design of smart home system based on ZigBee wireless sensor network. Aasri Procedia, Vol. 8, pp. 75–81. DOI: 10.1016/j.aasri.2014.08.013.
21. **Withanage, C., Ashok, R., Yuen, C., Otto, K. (2014).** A comparison of the popular home automation technologies. IEEE Innovative Smart Grid Technologies-Asia (ISGT ASIA), IEEE, 2014, pp. 600–605. DOI: 10.1109/ISGT-ASIA.2014.6873860.

*Article received on 23/02/2021; accepted on 24/03/2021.  
Corresponding author is Rafael Guzmán Cabrera.*